Chemical Engineering Journal 144 (2008) 336–342

Contents lists available at ScienceDirect

Chemical Engineering Journal

journal homepage: www.elsevier.com/locate/cej

Amine-modified ordered mesoporous silica: Effect of pore size on carbon dioxide capture

V. Zeleňák[a,*], M. Badaničová[a], D. Halamová[a], J. Čejka[b], A. Zukal[b], N. Murafa[c], G. Goerigk[d]

[a] Department of Inorganic Chemistry, P.J. Šafárik University, Moyzesova 11, 04154 Košice, Slovak Republic
[b] J. Heyrovský Institute of Physical Chemistry, v.v.i., Academy of Sciences of the Czech Republic, Dolejškova 3, CZ-182 23 Prague 8, Czech Republic
[c] Institute of Inorganic Chemistry, v.v.i., Academy of Sciences of the Czech Republic, 250 68 Řež, Czech Republic
[d] Hasylab, DESY, Notkestrasse 85, Hamburg, Germany

ARTICLE INFO

Article history:
Received 31 January 2008
Received in revised form 8 July 2008
Accepted 14 July 2008

Keywords:
Mesoporous silica
Hexagonal
Amine
Carbon dioxide
MCM
SBA

ABSTRACT

Three mesoporous silica materials with different pore sizes (33 Å for small pore size MCM-41; 38 Å for SBA-12; 71 Å for large pore size SBA-15) and pore connectivity (2D for MCM-41 and SBA-15-type materials; 3D for SBA-12 material) were prepared and functionalized with aminopropyl (AP) ligands by post-synthesis treatment. The materials were characterized by small angle X-ray scattering (SAXS), transmission electron microscopy (TEM), thermogravimetric analysis (TGA) and nitrogen adsorption/desorption experiments. The carbon dioxide sorption on modified mesoporous molecular sieves was investigated by using of microbalances at 25 °C, and the influence of pore size and pore architecture on CO_2 sorption was discussed. The large pore silica, SBA-15, showed the largest carbon dioxide sorption capacity (1.5 mmol/g), relating to highest amine surface density in this material. On the other hand, three-dimensional accessibility of amine sites inside the pores of SBA-12 silica resulted in a faster response to CO_2 uptake in comparison with MCM-41 and SBA-15 molecular sieves.

1. Introduction

The periodic mesoporous silica materials prepared using self-organized aggregates of surfactants are of current interest in modern nanomaterials chemistry. The self-assembly approach allows an adjustment of properties of new materials on nanoscale level by a change in the size and structure of surfactant aggregates. The assembly of surfactant molecules was at first applied in 1992 in the synthesis of mesoporous silica MCM-41 [1], and from this time the research of periodic mesoporous materials accelerated. The main research interests focused on the use of non-ionic surfactants or ionic liquids for the synthesis [2–4], characterization of materials by advanced techniques [5,6], and on potential applications of new materials in adsorption or catalysis [7–11].

The properties of mesoporous silica can be easily tailored by surface modification to prepare materials with desired properties and applications. In our work we are interested in use of the ordered mesoporous silica materials for capture and separation of greenhouse gases, notably carbon dioxide. Since carbon dioxide is an acidic gas, the grafting of basic centers, e.g. amines on the surface of the mesoporous silica can lead to preferential sorption of carbon dioxide by the modified materials. Amine active sites bonded on the surface of mesoporous solid can capture carbon dioxide through the formation of carbamates and carbonates, and such way to resemble the technological process of CO_2 scrubbing by liquid alkanolamines [12]. The new amine modified mesoporous solid sorbents could take advantage of high selectivity to carbon dioxide capture together with high gas flux and mass transfer within mesoporous solid. The successful use of solid amine sorbents can be already found in spacecraft technology, where the amine beds are used for removal of surplus carbon dioxide from closed environments in space shuttles or submarines [13].

The concept of carbon dioxide adsorption by amine-modified silica appeared in 1995, when Leal et al. [14] prepared amine-modified silica gel and studied carbon dioxide adsorption on this material. The adsorption capacity of the prepared material was below the requirement for industrial application. This concept revived at the beginning of this century in combination with periodic mesoporous silica. Xu et al. modified MCM-41 mesoporous silica with branched polyethylenimine (PEI) polymer containing numerous amine sites. They found that CO_2 adsorption capacity of MCM-41-PEI sample was much higher than that of the MCM-41 and about two times that of the pure PEI [15–17]. Group of Sayari studied conventional and pore-expanded MCM-41 silica modified with diamines and triamines. They showed that higher adsorption capacities were observed with pore-expanded MCM-41

* Corresponding author.
E-mail address: vladimir.zelenak@upjs.sk (V. Zeleňák).

1385-8947/$ – see front matter © 2008 Elsevier B.V. All rights reserved.
doi:10.1016/j.cej.2008.07.025

since the pore-expanded silica was able to accommodate a larger quantity of aminosilanes still allowing high adsorbate mobility [18–20].

Another member of MCM family, cubic MCM-48 silica, was studied in works of Huang et al. [21] and Kim et al. [22]. Huang et al. studied the adsorption properties of MCM-48 grafted by 3-aminopropyltriethoxysilane (APS). The adsorption capacities in dry conditions were determined as 1.14 mmol/g. When the sorbent was exposed to a humid stream of 5% CO_2/N_2, the adsorption capacity for CO_2 doubled [21]. Several types of amine groups attached on the surface of MCM-48 were studied by Kim et al. [22]. They used aminopropyl (monomeric, unhindered), pyrrolidinepropyl (monomeric, hindered), polymerized aminopropyl (polymeric, unhindered) and polyethylenimine (polymeric, hindered) amines for the study. MCM-48 silica containing polymeric amines showed higher concentration of amine sites but the monomeric aminopropyl-attached MCM-48 silica displayed higher CO_2 adsorption rate because of greater accessibility of amine adsorption sites.

Carbon dioxide sorption over SBA-15 silica was also studied in several works. The infrared study of CO_2 sorption on monoamine and diamine modified SBA-15 silica confirmed carbamate and carbonate as products of CO_2 chemisorption on these materials [23–25]. In works of Hiyoshi et al. [26,27] SBA-15 mesoporous silica was grafted by various aminosilanes, namely aminopropyltriethoxysilane, *N*-(2-aminoethyl)-3-aminopropyltrimethoxysilane (AEAPS), (3-trimethoxysilylpropyl)diethylenetriamine (TA). The efficiencies of the aminosilanes at identical surface density of amine were found to be in the order APS > AEAPS > TA.

A series of diethylenetriamine[propyl(silyl)] (DT) functionalized hexagonal mesoporous silicas were prepared by Knowles et al. [28,29]. The DT-functionalized materials were found to have greater CO_2 adsorption capacities than the analogous aminopropylsilyl (AP) and ethylenediamine[propyl-(silyl)] (ED) functionalized materials, but lower amine efficiencies.

Both MCM-41 and SBA-15 materials modified by *N*-β-(aminoethyl)-γ-aminopropyl dimethoxy methylsilane were studied by Zhao et al. [30]. They suggest that there are two contributions to carbon dioxide sorption on amine-modified mesoporous silica: the chemical adsorption based on the active sites of amine groups and the capillary condensation caused by the nanoscale channels of the mesoporous materials.

Different approach to the capture was described by Srivastava et al. [31,32]. They used amine-modified SBA-15 to transform carbon dioxide into technologically useful chemicals.

It can be seen from the literature overview that several works dealt with the study of effect of different amines on carbon dioxide sorption. However, the works dealing with the comparison of different materials and their influence of carbon dioxide sorption are scarce [18,19,30]. Therefore in the present study we have functionalized three mesoporous silica materials with different pore sizes (33 Å for MCM-41, 38 Å for SBA-12 and 71 Å for SBA-15 material) and different spatial pore system (2D for MCM-41 and SBA-15 materials and 3D for SBA-12 material) with 3-aminopropyl moieties and we have investigated carbon dioxide sorption over the materials.

2. Experimental

2.1. Synthesis and functionalization of mesoporous silicas

Mesoporous silicas MCM-41 and SBA-15 were synthesized by conventional procedures using ionic cetyltrimethylammonium bromide (CTAB) or triblock copolymer Pluronic P123 ($(EO)_{20}(PO)_{70}(EO)_{20}$) surfactants, respectively [1,2]. The synthesis of hexagonal silica SBA-12 was made using alkylethyleneoxide Brij76 ($C_{18}EO_{10}$) surfactant [2] by a modified procedure.

MCM-41 silica was prepared using low surfactant concentration at room temperature. The H_2O/NH_4OH/CTAB/TEOS molar ratio was 525/69/0.125/1. In a typical synthesis 205 ml of NH_4OH (25 wt.% solution) were mixed with 270 ml of distilled water. Then 2.0 g of surfactant were added into this solution with stirring. When the solution became homogenous, 10 ml of TEOS were added and the reaction mixture was stirred for 2 h. After this time the white solid product was filtered, washed with distilled water and dried at ambient temperature. The calcination was performed at 550 °C for 4 h.

For preparation of SBA-15, a typical gel composition in terms of molar ratio was TEOS/HCl/H_2O/P123 = 1/5.9/193/0.017. A portion of 4.0 g of Pluronic P-123 was dissolved with stirring in a mixture of 30 g of water and 120 g of 2 M HCl at 35 °C and 8.5 g of TEOS was then added. The resulting mixture was stirred at 35 °C for 20 h and then was aged at 80 °C for 24 h. The as-synthesized sample was recovered by filtration and freely dried. The organic template was removed by calcination in air at 500 °C for 7 h.

For the preparation of SBA-12, Brij 76 was first mixed with water and hydrochloric acid. The mixture was heated to 50 °C and stirred for 1 h at this temperature. After 1 h tetraethoxysilane was added under vigorous stirring. The resulting mixture was kept stirring for 1 day at 50 °C. The solid product was filtered off, repeatedly washed with distilled water and dried at room temperature. The HCl/H2O/Brij 76/TEOS molar ratio was 26.65/910.6/1/7.34. The surfactant was removed by calcination in air flow at 500 °C for 5 h.

The surface modification of the prepared mesoporous silicas by 3-aminopropyl groups was carried out by grafting in dried toluene using 3-aminopropyltriethoxysilane as amine source. Prior to the grafting the mesoporous silicas were dehydrated at 200 °C for 3 h to remove adsorbed moisture. Then 1 g of the respective mesoporous silica was dispersed in 50 cm^3 of dried toluene and 3 cm^3 of AP were added to the suspension, which was further kept under reflux for 20 h. The solid product was recovered by filtration, repeatedly washed out with toluene and octane and dried overnight at 80 °C.

2.2. Characterization

Small angle X-ray scattering (SAXS) experiments were carried out at B1/Jusifa Hasylab beamline (DESY Hamburg) with the beam energy 12 keV (λ = 1.03 Å). The HRTEM micrographs were recorded on a JEOL JEM 3010 microscope. Thermal stability of the samples and carbon dioxide sorption tests were carried out by using of STA Netzch 409PC apparatus. Thermal characterization was carried out under dynamic conditions with heating rate 9 °C/min in atmosphere of air (20 cm^3/min). Carbon dioxide sorption was investigated at 25 °C. Before the sorption experiments the samples were first activated by heating in inert gas (Ar) at 110 °C to remove preadsorbed carbon dioxide and water. After 30-min isothermal step at this temperature, the sample was cooled down to 25 °C and kept isothermally at this temperature for 1 h. During this time the temperature and TG signals were stabilized. When the purge gas was switched to 10% CO_2/N_2 mixture (flow rate 20 cm^3/min) and weight gain was recorded by thermobalances. The 10% CO_2/N_2 certified gas mixture was purchased from Linde gas.

Nitrogen adsorption/desorption experiments were performed with a Quantachrome autosorb automated gas sorption system at 77 K. Prior to the experiments the samples were outgassed at 393 K for 8 h.

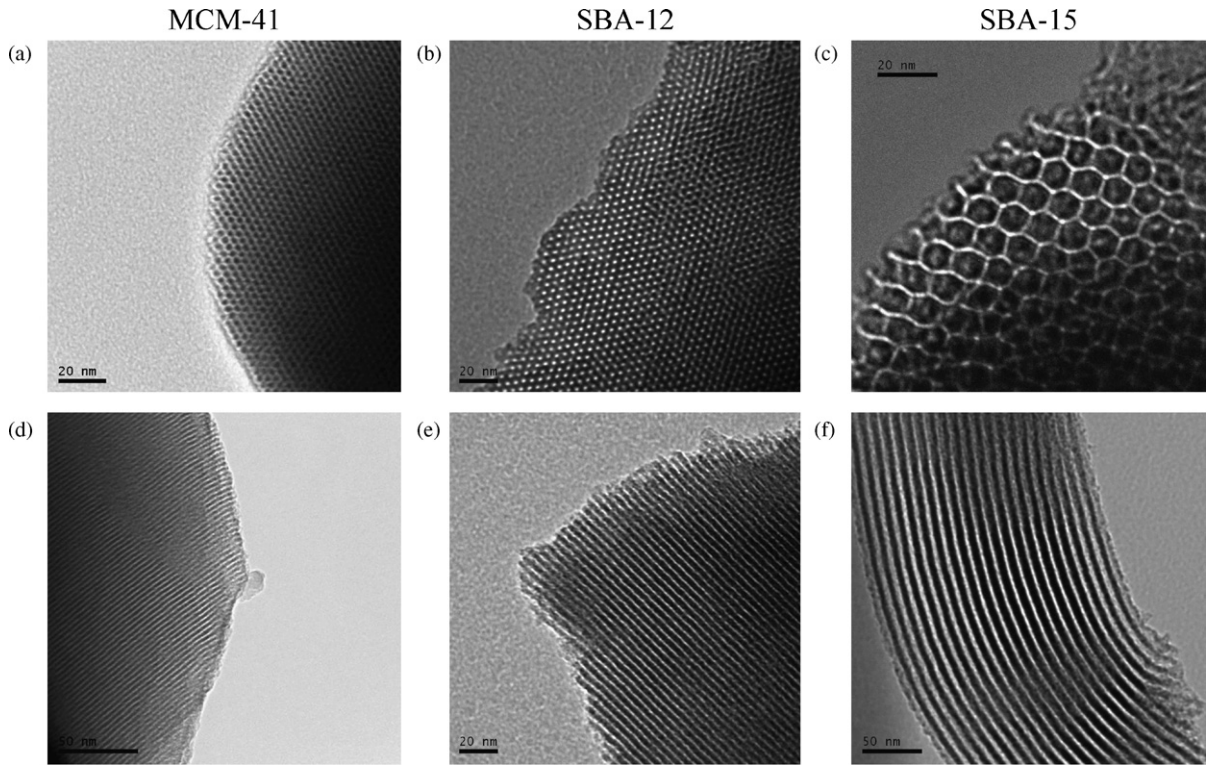

Fig. 1. HRTEM micrographs of MCM-41 (a), SBA-12 (b), SBA-15 (c) viewed along the hexagonal axis and MCM-41 (d), SBA-12 (e), SBA-15 (f) viewed perpendicular hexagonal axis.

3. Results and discussion

Figs. 1 and 2 show HRTEM micrographs and SAXS patterns of the calcined mesoporous silica MCM-41, SBA-12 and SBA-15. Well-ordered mesoporous structures of hexagonal symmetry with alternating channels and siliceous framework can be seen in Fig. 1 for MCM-41 and SBA-15 materials. For the SBA-12 material the hexagonal pore arrangement is suggested by HRTEM micrographs. However it is known, that the intergrowth of hexagonal close-packed (hcp) and cubic close-packed (ccp) structure is typical for SBA-12 silica [6,33]. Therefore the micrographs of SBA-12 sample can either be a signature of the hexagonal structure viewed along $[0\,0\,1]_H$, or of a cubic viewed along $[1\,1\,1]_C$. It is not possible to distinguish between these two phases from HRTEM, since we do not have ED patterns. Moreover, the SAXS study (see further in the text) did not answer this question as well. The mean pore size as determined by transmission electron microscopy (TEM) is about 3 nm for the MCM-41 sample, 3.5 nm for the SBA-12 sample and 7.5 nm for the SBA-15 sample. These data are in a good agreement with pore sizes determined from nitrogen adsorption isotherms.

The long-range ordering of the prepared materials was reflected also by SAXS measurements (see Fig. 2). The SAXS pattern of MCM-41 silica exhibits a strong diffraction peak at $q = 0.186\,\text{Å}^{-1}$ and the weak ones at $q = 0.322$, 0.372 and $0.482\,\text{Å}^{-1}$ (Fig. 2a upper line) corresponding to d-spacings 34.7, 19.5, 16.9 and 13.0 Å. The SBA-15 material was characterized by four diffraction profiles with $q = 0.06$, 0.104, 0,121 and $0.161\,\text{Å}^{-1}$ (Fig. 2c upper line), with corresponding d-spacing 104.7, 60.4, 51.9 and 39.0 Å. The unit cell parameter a, which was calculated from the (1 0) diffraction peak according to the equation $a = 2 \times d_{10}/\sqrt{3}$, is 40.1 Å for MCM-41 material and 120.9 Å for the SBA-15 material. For SBA-12 silica, only one peak with $q = 0.138\,\text{Å}^{-1}$ was observed in the SAXS experiment. Due to presence of only this peak, the unequivocal assignment of the symmetry from SAXS pattern is not possible since polytypic intergrowth of hexagonal close-packed (hcp) and cubic close-packed (ccp) structure can occur [6,33]. So, diffraction peak in pattern of

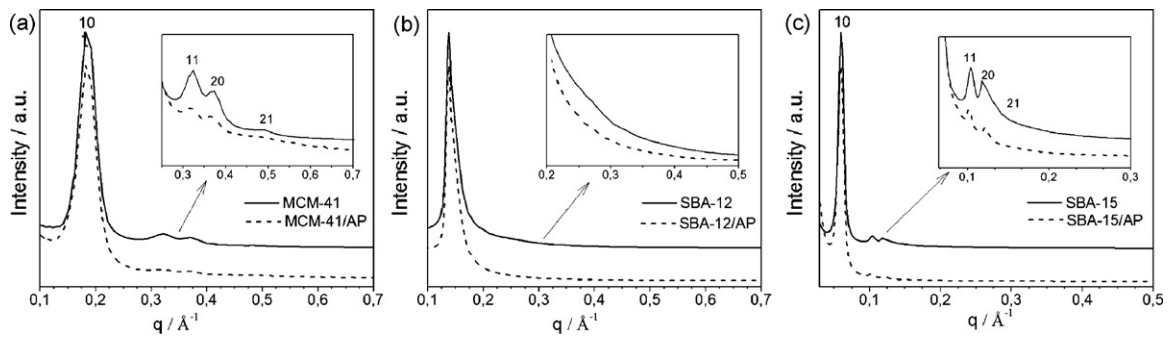

Fig. 2. SAXS patterns of unmodified (solid line) and aminopropyl-modified (dashed line) mesoporous silica MCM-41 (a), SBA-12 (b) and SBA-15 (c).

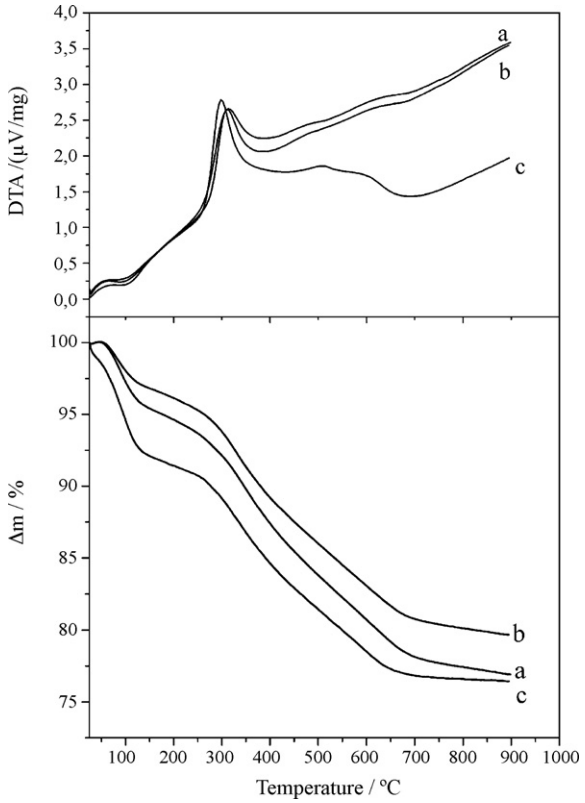

Fig. 3. TG/DTA curves of the samples (a) MCM-41/AP, (b) SBA-12/AP and (c) SBA-15/AP.

SBA-12 could be corresponded to (0 0 2) plane of hcp or (1 1 1) plane of ccp structure.

The SAXS measurements of the modified materials showed that long-range ordering of the materials was retained after modification (Fig. 2a–c, bottom lines). The decrease in the intensities of diffraction lines was observed in the aminopropyl-modified silicas. The SAXS diffraction profiles of the grafted molecular sieves occur at same angles in comparison with pure silicas indicating no substantive change of the mesoporous matrix after silanization treatments.

The quantification of the 3-aminopropyl loading into mesoporous matrix was made by thermogravimetric analysis (TG/DTA, see Fig. 3) on heating in air. Two main steps were observed on the TG curves of the modified materials. The first step takes place in the temperature range 25–200 °C and the second one in the temperature range 200–700 °C. The mass loss up to 200 °C corresponds to liberation of pre-adsorbed water and carbon dioxide. The large-pore silica SBA-15 showed the highest mass loss in this temperature range, suggesting that pores of this material are more accessible to these molecules in comparison with the other two silicas.

The second step of thermal decomposition, in the range 200–700 °C, corresponds to the decomposition of 3-aminopropyl ligands. The dehydroxylation, which may occur in this temperature range, could be neglected, since the sample was pre-dried before grafting and dry anhydrous solvents, kept over molecular sieves, were used in the synthesis. As shown by Huang et al. [21] free surface hydroxyl groups react with siloxane during grafting in anhydrous solvents. Moreover, the "dangling" (non-hydrolyzed) alkoxy groups, which could potentially account to the mass loss observed on TG curve, are removed below 200 °C as it was confirmed by Sayari and co-worker [20]. Therefore the total weight loss beyond 200 °C is due to decomposition of grafted amine ligands [20].

The mass loss observed in the temperature range 200–700 °C was 16.5% for the sample MCM-41/AP, 15.2% for the sample SBA-12/AP and 14.2% for the sample SBA-15/AP, which correspond to 3.00, 2.76 and 2.72 mmol of AP (or $-NH_2$ adsorption sites) per gram of silica respectively. It is obvious that similar weight loadings were achieved for all three silica samples. However, as it will be shown further in the text, the grafting density, which is expressed as the amount of $-NH_2$ groups per 1 nm^2 of the mesoporous silica support, differ for the particular samples (see Table 1).

The chemical reaction (chemisorption) between amine active sites and carbon dioxide is the driving force for the sorption of carbon dioxide by amine-modified silica materials, yielding carbamate in anhydrous conditions

$$CO_2 + 2R\text{–}NH_2 \rightarrow RNH_3^+ + R\text{–}NHCOO^- \quad (1)$$

Since the reaction involves two nitrogen atoms of amine groups two nitrogen atoms in close proximity are required on the surface. As published by Hiyoshi et al. [27], the isolated amine groups are ineffective in CO_2 capture.

The textural characteristics of the samples were determined by nitrogen adsorption/desorption. The N_2 adsorption isotherms of unmodified and aminopropyl-modified samples are shown in Fig. 4. The surface area of all materials under study was evaluated using BET method. The pore size distribution was calculated using standard NLDFT approach (isotherms without hysteresis) or BJH method (isotherms with hysteresis). The nitrogen adsorption/desorption isotherm of the sample MCM-41 (Fig. 4a) is of the type IV in the IUPAC classification with a sharp step over a narrow range of relative pressure (P/P_0 = 0.2–0.35) arising from the capillary condensation of nitrogen in the mesopores. BET surface area of MCM-41 sample was 1506 m^2/g and pore diameter was about 33 Å (see inset of Fig. 4a). The external surface area, determined by t-method was 52 m^2/g. Similarly to MCM-41, the N_2 adsorption–desorption isotherm of SBA-12 sample (Fig. 4b) is of type IV without hysteresis. The initial part of the adsorption isotherm corresponds to the adsorption on the mesopore surface. The isotherm shows a well-defined step in the adsorption and desorption curve between partial pressures P/P_0 of 0.2–0.4, indicative of the filling of mesopores. The average pore size of the SBA-12 was about 38 Å (Fig. 4b, inset), BET and external surface areas were 1347 and 37 m^2/g, respectively. The adsorption/desorption isotherm of the sample SBA-15 is characterized by the hysteresis loop. Mesopores filling step occurs between P/P_0 = 0.68–0.75 (see Fig. 4c). Desorption from the sample SBA-15 is delayed and the evaporation step occurs in the range of P/P_0 = 0.58–0.66. BET surface area of

Table 1
Textural properties of the unmodified and modified periodic silica samples

Sample notation	Surface area (m^2/g)	External surface area (m^2/g)	Pore size (Å)	Amine loading (mmol/g)	Amine surface density NH_2 (group/nm^2)
MCM-41	1506	52	33	–	–
MCM-41/AP	239	38	18	3.00	1.1
SBA-12	1347	37	38	–	–
SBA-12/AP	310	9	27	2.76	1.2
SBA-15	687	55	71	–	–
SBA-15/AP	134	28	56	2.72	2.4

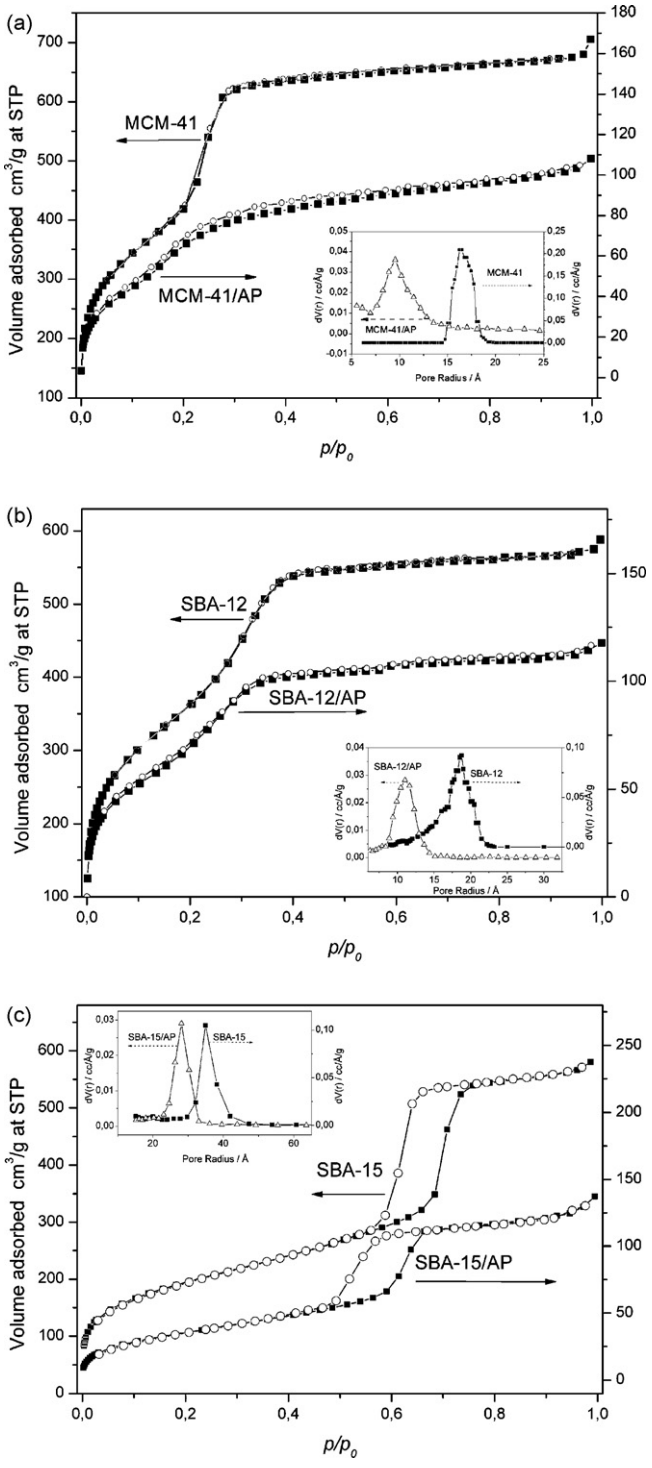

Fig. 4. Nitrogen adsorption/desorption isotherms and pore size distribution of the samples (a) MCM41 and MCM-41/AP, (b) SBA-12 and SBA-12/AP (c) SBA-15 and SBA-15/AP.

SBA-15 sample is 687 m^2/g, external surface area 55 m^2/g and the average mesopore size of 71 Å (Fig. 4c, inset).

The specific surface areas were found to decrease significantly upon functionalization. The mesoporous adsorption step in the modified sample MCM-41/AP is much less resolved than in parent MCM-41 due to filling of mesopores by aminopropyl ligands. The BET surface area of modified sample decreased to 239 m^2/g, external surface area to 38 m^2/g and pore size to 18 Å. Such significant decrease of textural properties for small-pore materials was also described by Walcarius et al. [34]. For SBA-12 material with the 3D pore architecture and slightly larger pore size than MCM-41 the mesoporous adsorption step is better resolved after functionalization. The sample SBA-12/AP has pore size in the mesoporous region (27 Å). The BET surface area of this sample was 310 m^2/g and external surface area 9 m^2/g. The nitrogen adsorption/desorption measurements for large-pore SBA-15 material showed, that even the pore size and specific area (134 m^2/g) decreased upon modification by 3-aminopropyl ligands, the pores are still large enough (56 Å) for adsorbate to diffuse easy within the channels. The external surface area in SBA-15/AP was 28 m^2/g. Low external surface areas in both parent mesoporous molecular sieves as well as in modified samples show, that amines are bound mainly on the inner surface of the materials. The textural properties of the materials are summarized in Table 1.

Carbon dioxide uptake on amine-modified molecular sieves is driven by chemisorption, the reaction between carbon dioxide as an acidic gas and basic nitrogen active sites, yielding carbamates (see Eq. (1)). In presence of water the carbamate can further react giving bicarbonate. In any case, according to Dankwerts' mechanism amine pair is required for the reaction [35]. Therefore isolated amine groups are less effective in chemisorption of carbon dioxide and densely anchored aminosilane are more efficient [27]. In this sense, the key parameter influencing the carbon dioxide sorption by amine-modified materials is not surface area, but density of $–NH_2$ active sites on the surface of the support. When we take into account the amine loading determined by the thermogravimetric analysis and surface area of parent mesoporous support, we can determine the statistical surface densities of amines in the modified samples. These densities are 1.1 $–NH_2$ groups/nm^2 for MCM-41/AP sample, 1.2 $–NH_2$ groups/nm^2 for SBA-12/AP sample and 2.4 $–NH_2$ groups/nm^2 for SBA-15/AP sample. The highest sorption capacity should be expected for the SBA-15/AP sample, while samples SBA-12/AP and MCM-41/AP should have sorption capacity similar but lower than SBA-15/AP.

The CO_2 sorption capacity was measured by microbalances at 25 °C (see Fig. 5). Flow of carbon dioxide over the samples led to a weight gain and evolution of heat as reflected by TG and DTA curves, respectively. The total amount of sorbed CO_2 was 0.57 mmol/g for sample MCM-41/AP, 1.04 mmol/g for sample SBA-12/AP and 1.54 mmol/g for the sample SBA-15/AP. It is obvious that the largest adsorption capacity was determined for SBA-15/AP sample, which is in accordance with highest amine surface density in this material. The determined sorption capacity for SBA-15/AP sample is higher than reported for similar materials by Hyoshi et al. [27]. However, the capacity is below the values observed by Sayari et al. for pore-expanded silica modified by triamine, showing sorption capacity 2.65 mmol/g [20]. Different sorption capacities were observed for SBA-12/AP and MCM-41/AP samples although both of them have similar amine surface densities. This suggests that the amine surface density is not the only parameter influencing the carbon dioxide sorption in these materials. Another parameter influencing the sorption capacity is pore size. Sayari et al. showed [20], that large pore mesoporous silica MCM-41 has higher carbon dioxide sorption capacity than conventional one. As evidenced by nitrogen adsorption/desorption measurements, the pores of MCM-41/AP are filled and therefore a certain amount of the pores may be blocked and inaccessible for gas molecules, resulting in low CO_2 sorption capacity. The pores of SBA-12/AP (27 Å) are larger than in MCM-41/AP and moreover, the SBA-12 silica has 3D pore architecture, which can make the gas flow into the material to be easier. Three-dimensional accessibility of adsorption sites in SBA-12/AP sample together with its larger pore size results in higher sorption capacity of this material in comparison with MCM-41/AP sample.

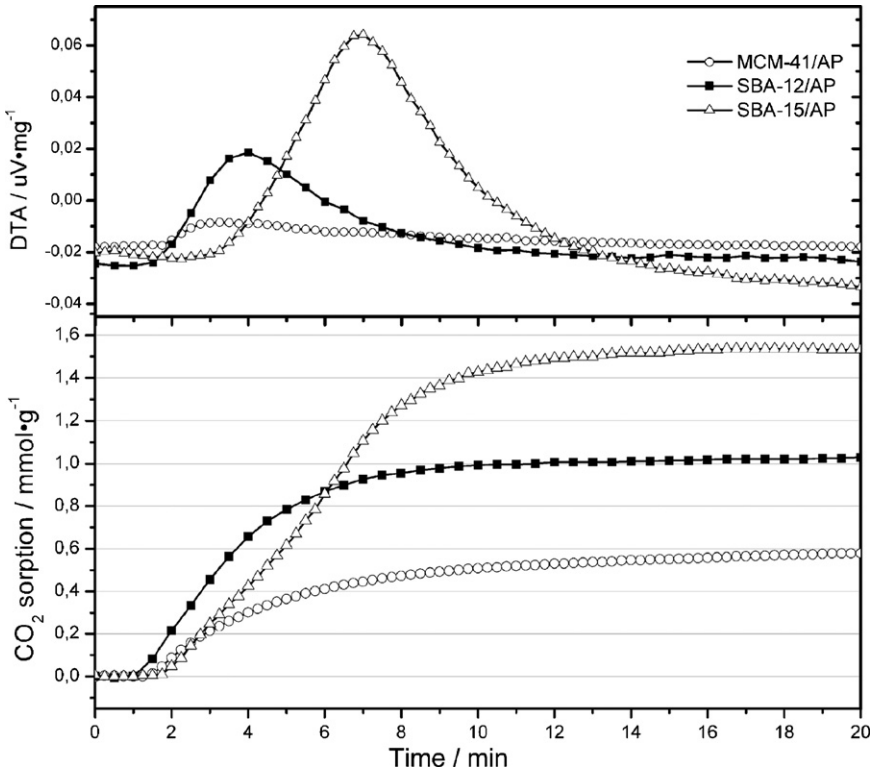

Fig. 5. Carbon dioxide sorption over the samples MCM-41/AP (circles), SBA-12/AP (squares) SBA-15/AP (triangles).

Finally, high amine surface density of SBA-15/AP, together with its large pore size (56 Å) leads to the highest carbon dioxide uptake from all three samples. It should be noted, that the cumulative weight change, i.e. onset of the carbon dioxide uptake for SBA-12/AP material was registered sooner than for the other two samples (see Fig. 5). It can indicate that three-dimensional accessibility of amine sites inside the pores of SBA-12 silica resulted in a faster response to CO_2 uptake in comparison with MCM-41 and SBA-15 molecular sieves.

4. Conclusions

Three amine-modified silica molecular sieves were tested as sorbents for carbon dioxide capture. The sorption capacity was found to depend on the surface density of amine groups and on the pore size of the mesoporous silica. The molecular sieves with larger pores and higher surface density of amines possess higher sorption capacity. The lower limit for pore size of mesoporous silicas to be used in preparation of efficient amine-based sorbents is approximately 35 Å. Below this size of pores the amine adsorption sites inside the pores are inaccessible for CO_2 molecules due to their limited diffusion into the pores. The sooner onset of carbon dioxide uptake observed for SBA-12/AP, which might reflect three-dimensional accessibility of amine active sites in this material.

Acknowledgements

This work was supported by European Community STREP project "DeSANNS" (No. FP6-SES6-020133)), the Slovak Research and Development Agency under the contract no. RPEU-0027-06 (OrNaMat), MVTS6 and VEGA (No. 1/0119/08) projects of Ministry of Education of the Slovak Republic. J.Č. and A.Z. acknowledge the Grant Agency of the Czech Republic (No. 203/08/0604) for the financial support. The TEM micrograph measurements were kindly supported by the Project 1M4531477201 of Ministry of Youth and Sports of the Czech Republic.

References

[1] J.S. Beck, J.C. Vartuli, W.J. Roth, M.E. Leonowicz, C.T. Kresge, K.D. Schmitt, C.T.W. Chu, D.H. Olson, E.W. Sheppard, S.B. McCullen, J.B. Higgins, J.L. Schlenker, J. Am. Chem. Soc. 114 (1992) 10834–110834.
[2] D. Zhao, Q. Huo, J. Feng, B.F. Chmelka, G.D. Stucky, J. Am. Chem. Soc. 120 (1998) 6024–6036.
[3] A. Zukal, M. Thommes, J. Čejka, Micropor. Mesopor. Mater. 104 (2007) 52–58.
[4] N. Žilková, A. Zukal, J. Čejka, Micropor. Mesopor. Mater. 95 (2006) 176–179.
[5] Y. Sakamoto, M. Kaneda, O. Terasaki, D.Y. Zhao, J.M. Kim, G. Stucky, H.J. Shin, R. Ryoo, Nature 408 (2000) 449–453.
[6] Y. Sakamoto, I. Diaz, O. Terasaki, D. Zhao, J. Perez-Pariente, J.M. Kim, G.D. Stucky, J. Phys. Chem. B 106 (2002) 3118–3123.
[7] D. On, D. Desplantiers-Giscard, C. Danumah, S. Kaliaguine, Appl. Catal. A 222 (2001) 299–357.
[8] M.J. Jia, W.R. Thiel, Chem. Commun. (2002) 2392–2393.
[9] M. Vicevic, K.V.K. Boodhoo, K. Scott, Chem. Eng. J. 133 (2007) 31–41.
[10] J. Demel, P. Štěpnička, J. Čejka, J. Mol. Catal. A 274 (2007) 127–132.
[11] J.A. Melero, G. Calleja, F. Martínez, R. Molina, M.I. Pariente, Chem. Eng. J. 131 (2007) 245–256.
[12] E. Rinker, S.S. Ashour, O.C. Sandall, Ind. Eng. Chem. Res. 39 (2000) 4346–4356.
[13] S. Satyapal, T. Filburn, J. Trela, J. Strange, Energy Fuels 15 (2001) 250–255.
[14] O. Leal, C. Bolivar, C. Ovalles, J.J. Garcia, Y. Espidel, Inorg. Chim. Acta 240 (1995) 183–189.
[15] X. Xu, Ch. Song, J.M. Andresen, B.G. Miller, A.W. Scaroni, Energy Fuels 16 (2002) 1463–1469.
[16] X. Xu, Ch. Song, J.M. Andresen, B.G. Miller, A.W. Scaroni, Micropor. Mesopor. Mater. 62 (2003) 29–45.
[17] X. Xu, Ch. Song, B.G. Miller, A.W. Scaroni, Fuel Process. Technol. 86 (2005) 1457–1472.
[18] R.S. Franchi, P.J.E. Harlick, A. Sayari, Ind. Eng. Chem. Res. 44 (2005) 8007–8013.
[19] P.J.E. Harlick, A. Sayari, Ind. Eng. Chem. Res. 45 (2006) 3248–3255.
[20] P.J.E. Harlick, A. Sayari, Ind. Eng. Chem. Res. 46 (2007) 446–458.
[21] H.Y. Huang, R.T. Yang, D. Chinn, C.L. Munson, Ind. Eng. Chem. Res. 42 (2003) 2427–2433.
[22] S. Kim, J. Ida, V.V. Guliants, J.Y.S. Lin, J. Phys. Chem. B 109 (2005) 6287–6293.
[23] C.C. Chang, S.S.C. Chuang, M. Gray, Y. Soong, Energy Fuels 16 (2003) 468–473.
[24] R.A. Khatri, S.S.C. Chuang, Y. Soong, M. Gray, Ind. Eng. Chem. Res. 44 (2005) 3702–3708.
[25] R.A. Khatri, S.S.C. Chuang, Y. Soong, M. Gray, Energy Fuels 20 (2006) 1514–1520.

[26] N. Hiyoshi, K. Yogo, T. Yashima, Micropor. Mesopor. Mater. 84 (2005) 357–365.
[27] N. Hiyoshi, K. Yogo, T. Yashima, Chem. Lett. 33 (2004) 510–511.
[28] G.P. Knowles, S.W. Delaney, A.L. Chaffee, Ind. Eng. Chem. Res. 45 (2006) 2626–2633.
[29] G.P. Knowles, J.V. Graham, S.W. Delaney, A.L. Chaffee, Fuel Proc. Technol. 86 (2005) 1435–1448.
[30] H. Zhao, J. Hu, J. Wang, L. Zhou, H. Liu, Acta Phys. Chim. Sin. 23 (2007) 801–806.
[31] R. Srivastava, D. Srinivas, P. Ratnasamy, J. Catal. 233 (2005) 1–15.
[32] R. Srivastava, D. Srinivas, P. Ratnasamy, Micropor. Mesopor. Mater. 90 (2006) 314–326.
[33] S.B. Jung, Ch.K. Han, H.H. Park, Appl. Surf. Sci. 244 (2005) 47–50.
[34] A. Walcarius, M. Etienne, B. Lebeau, Chem. Mater. 15 (2003) 2161–2173.
[35] P.V. Dankwerts, Chem. Eng. Sci. 34 (1979) 443–445.